International Journal of Automotive Technology, Vol. 8, No. 2, pp. 149–154 (2007)

1229-9138/2007/033-03

NUMERICAL ANALYSIS OF A SAMPLING MODULE FOR A FAST RESPONSE EXHAUST GAS ANALYZER

W. S. KIM[1)], J. H. LEE[2)], J. S. YOO[2)], B. O. RHEE[2)] and J. I. PARK[2)*]

[1)]Hyundai Motor Company, 772-1 Jangduk-dong, Hwaseong-si, Gyeonggi 445-706, Korea
[2)]School of Mechanical Engineering, Ajou University, Gyeonggi 443-749, Korea

(Received 14 February 2006; Revised 9 February 2007)

ABSTRACT–The engine behavior in a transient condition is important to not only emission regulations but also fuel economy. A fast response gas analyzer can be a useful tool to investigate exhaust gas in a transient operation. It should be designed to analyze gas concentration with a short time constant by a fast sampling module and an appropriate measuring method for each emission element. In this study, a new fast sampling module is introduced and flow analysis is performed by numerical simulation. The analysis has shown the proper operating condition and the sensitivity of the module for practical application. Calculated flow to the sampling module has 0.5~4% error, while backflow toward the expansion tube is expected when pressure in CP (Constant Pressure) chamber is over 0.6 bar. For a stable supply of flow to the optical cell, sample gas pressure should be in the range, 0.35~1.90 bar, when the pressure in the CP camber and the optical cell are 0.2 bar and 0.158 bar, respectively.

KEY WORDS : Sampling module, Fast analyzing, Optical cell, Total response time

NOMENCLATURE

c : concentration of sample gas
I_o : intensity of infrared light emitted into the gas
k : kinetic energy of trubulence
L : length of sample cell
x, y, z : rectangular coordinates
u, v, w : velocity of rectangular coordinates
T_t : time for the sample gas to arrive at measuring point
α : absorbtion constant
ε : dissipation rate
τ : time for measure the concentration

SUBSCRIPT

i, j, k : axis in rectangular coordinates
j' : species of gas

1. INTRODUCTION

The transient behavior of an engine has been widely investigated due to strict regulations on harmful exhausts. A fast response concentration analyzer can be a useful tool to understand engine characteristics in a transient condition since it is fast enough to analyze exhaust gas cycle by cycle (Steula *et al.*, 2000; Green, 2000). In addition, it is used to detect various emission gases including unburned hydrocarbon, carbon dioxide, carbon monoxide, and nitrogen oxide simultaneously (Sergei *et al.*, 1998; Zhao and Ladommatos, 1999). One of the key technologies for the fast response analyzer is a sampling module which picks up exhaust gas and delivers it to the test section.

Peckham (1993) introduced a sampling module which consists of capillary tubes and extracts sample gas from a cylinder or exhaust manifold directly and applied it to a FRFID (Fast Response Flame Ionization Detector). Summers and Collings (1995) divided the fast sampling module into several parts such as transfer, expansion and FID tube, and analyzed flow in each part with simple models. They also estimated the response time for each part.

However, the response time for each part is not verified and has considerable error compared to experimental data, especially during a transient condition. Moreover, estimation of velocity and density of sampled gas in the sampling module is necessary to ensure measuring sensitivity and stability of the analyzer.

In this study, a new sampling module which allows fast sampling of objective gas is introduced and analyzed using a commercial code, FLUENT. Internal density, velocity and response time are calculated and compared with experiments (Kim, 2004; Lee *et al.*, 2006).

*Corresponding author. e-mail: jpark@ajou.ac.kr

2. THEORETICAL CONSIDERATION

2.1. Sampling Module

Exhaust gas should be extracted and supplied to a detector fast enough to ensure cycle by cycle measurements, but rapid movement in the module causes a choking and density decrease of the objective gas, resulting in sensitivity deterioration.

To solve these problems, the sample module is organized into a sample transfer tube, expansion tube, CP chamber, optical tube and optical cell as in Figure 1. The sampling module keeps the pressure of the optical cell lower than that of the CP chamber. The bleed line connected outside keeps the pressure difference between the two parts constant by controlling the amount of each gas discharged. Sampled gas is accelerated in a transfer tube and stabilized in an expansion tube. The expansion tube is designed to keep the gas pressure as low as the CP chamber's with decreasing velocity, so that the gas pressure at the inlet of the optical cell is similar to the CP chamber's, and the pressure difference between the inlet of the optical tube and the optical cell is maintained constant. Under these conditions, the distribution of velocity and density of sample gas in the whole module is calculated and the response time of the fast sampling module is estimated, which is essential to determine various design factors and the available operating range for the fast sampling module.

2.2. Organization of Concentration Detector

In order to measure response time, CO_2 is selected as sample gas, since it is one of the major components in exhaust gas. Detector parts are designed for CO_2 gas and NDIR (Non-Dispersive InfraRed) techniques are introduced, which are widely used for the analysis of CO_2 concentration. The techniques use a specific characteristic of a dipole molecule against an infrared ray; dipole molecules such as CO_2, CO, C_xH_y, NO_x, and H_2O absorb the energy at a certain wavelength when exposed to infrared rays. Therefore, the energy of infrared rays decreases in the specific wavelength after passing through the molecules. Lambert-Beer's Law used in NDIR techniques is summarized below.

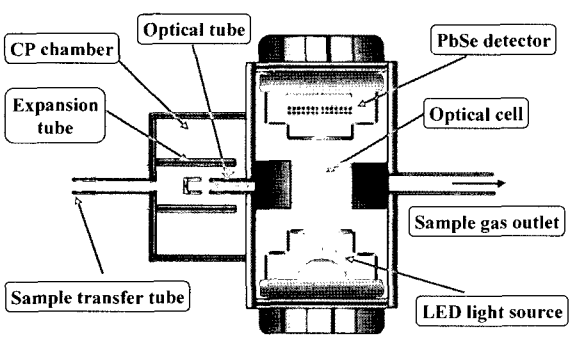

Figure 1. Schematic diagram of the fast sampling module.

$$I=I_o\times e^{-\alpha\times c\times L} \tag{1}$$

The sensitivity can be expressed in Equation (2) by differentiating Equation (1).

$$\frac{dI/I}{dc/c}=-\alpha\times c\times L \tag{2}$$

A difference of voltage on a detector indicates CO_2 concentration since a difference in CO_2 concentration results in a difference of light intensity by the detector. An infrared light source and detector are mounted apart at the ends of the optical path, which allows light to pass through the sample cell. Since the analysis of concentration with NDIR techniques utilizes very small voltage change resulting from the variance of CO_2 concentration, attention should be paid to electrical noise and drift due to the variance in temperature. In order to minimize drifts due to temperature variance, TE-cooler with thermistor is installed, which is supposed to keep the temperature at 30 ± 0.01°C.

A mechanical chopper on a specific frequency is usually used to achieve a better S/N ratio, but in this experiment, a semiconductor laser with 1ms chopping frequency is selected as a light source in order to achieve fast response time. A PbSe type photo conductor is suitable for a detector that provides fast response time (<30 μsec) and sensitivity ($D^*=1.2\sim1.6\times10^{-8}$) at a certain infrared wavelength (4.28 μm).

3. NUMERICAL ANALYSIS OF SAMPLING MODULE

FLUENT is used to carry on three dimensional numerical analysis of flow pattern in the sampling module of the fast CO_2 concentration analyzer. FLUENT uses a standard k-ε turbulence model for a turbulent flow field and continuity equation, momentum equation, and an energy equation listed below, serving as governing equations of abnormal compressible flow.

$$\frac{\partial\rho}{\partial t}+\frac{\partial}{\partial x_i}(\rho u_i)=0 \tag{3}$$

$$\frac{\partial}{\partial t}(\rho u_i)+\frac{\partial}{\partial x_i}(\rho u_i u_j) =-\frac{\partial p}{\partial x_i}+\frac{\partial}{\partial x_j}\left\{\mu\left(\frac{\partial u_i}{\partial x_j}+\frac{\partial u_j}{\partial x_i}-\frac{2}{3}\frac{\partial u_k}{\partial x_k}\delta_{ij}\right)-\rho\overline{u_i' u_j'}\right\} \tag{4}$$

$$\frac{\partial}{\partial t}(\rho E)+\frac{\partial}{\partial x_i}(u_i(\rho E+p)) =\frac{\partial}{\partial x_i}\left(k_{eff}\frac{\partial T}{\partial x_i}-\sum_{j'}h_{j'}J_{j'}+u_j(\tau_{ij})_{eff}\right) \tag{5}$$

k_{eff} represents effective conductivity, and J_j is diffusion flux of species j'. E is described in equation below.

$$E=h-\frac{p}{\rho}+\frac{u_i^2}{2} \tag{6}$$

In turbulence flow, Reynolds stress ($\rho\overline{u_i' u_j'}$) is proportional to a gradient of mean velocity, and its proportional coefficient is μ_t. This assumption is known as Boussinesq's assumption, and described below.

$$\tau_i=-\rho\overline{u_i' u_j'}$$
$$=-\rho\frac{2}{3}k\delta_{ij}+\mu_t\left(\frac{\partial u_i}{\partial x_j}+\frac{\partial u_j}{\partial x_i}\right)-\frac{2}{3}\mu_t\frac{\partial u_k}{\partial_k}\delta_{ij} \tag{7}$$

In this study, standard k-ε is used to determine a turbulence viscosity coefficient. The governing equation for k, turbulence kinetic energy, and ε, dissipation rate, is described below.

$$\mu_k=\rho C_\mu\frac{k^2}{\varepsilon} \tag{8}$$

$$\frac{\partial}{\partial x_i}(\rho u_i k)=\frac{\partial}{\partial x_i}\left(\frac{u_t}{\sigma_k}\frac{\partial k}{\partial x_i}\right)+G_k-\rho\varepsilon \tag{9}$$

$$\frac{\partial}{\partial x_i}(\rho u_i \varepsilon)=\frac{\partial}{\partial x_i}\left(\frac{u_t}{\sigma_k}\frac{\partial \varepsilon}{\partial x_i}\right)+C_{1\varepsilon}G_k\frac{\varepsilon}{k}-C_{2\varepsilon}\rho\frac{\varepsilon^2}{k} \tag{10}$$

Here, coefficients $C_{1\varepsilon}$, $C_{2\varepsilon}$, C_μ, σ_k, and σ_ε are experimental constants, and G_k represents the generation of tubulence kinetic energy.

$$G_k=\mu\left(\frac{\partial u_i}{\partial x_i}+\frac{\partial u_i}{\partial x_j}\right)\frac{\partial u_i}{\partial x_i} \tag{11}$$

A species transport equation is used to calculate the distribution of CO_2 concentration in an abnormal state.

$$\frac{\partial}{\partial t}(\rho m_{i'})\frac{\partial}{\partial x_i}(\rho u_i m_{i'})=-\frac{\partial}{\partial x_i}J_{i',i} \tag{12}$$

Here, $J_{i',i}$ is the diffusion flux of species i'. The equation below describes $J_{i',i}$ in turbulent flow.

$$J_{i',i}=-\left(\rho D_{i',m}+\frac{\mu_t}{Sc_t}\right)\frac{\partial m_{i'}}{\partial x_i} \tag{13}$$

Sc_t in Equation (13) is the turbulent Schmidt Number, and $D_{i',m}$ is a diffusion coefficient of species i' in mixture.

The power law is used for differentiating the convection term, and the equation describing the relationship between velocity and pressure of momentum is determined by a SIMPLE algorithm and for better convergence and stability, an under-relaxation method is applied. Ideal gas assumption is used for the calculation of compressible flow. In the case of an unsteady calculation, an implicit time integral method is used, while solutions for each physical time interval are obtained through the internal repetition of the proper number of iterations, approximately 500, until the solution is acquired; this process is repeated over time.

4. INSTRUMENTS AND METHODS FOR EXPERIMENT

Results of the numerical analysis are verified by comparing with experiments. Figure 2 shows a test bench for measuring total response time with pressure variation. The total response time is defined as the time required for the sensor output to change by 90% of the real value.

In order to measure response time, N_2 gas flows into the module using a vacuum pump, then CO_2 gas is led to the module by a solenoid valve. The solenoid valve used in the module has a 6 ms delay when fully open, which is subtracted from a measured total response time, to calculate real response time. A laminar flow meter is used to measure mass flow rates toward the sampling module, respecting CP chamber pressure variation.

5. ANALYSIS AND EXPERIMENTAL RESULTS

5.1. Numerical Results

Figure 3 shows output of FLUENT analysis with the following boundary conditions: CP Chamber - 0.5 bar, Optical cell - 0.4 bar, which is determined before developing the actual sampling module. CO_2 gas is accelerated up to 160 m/s when the gas passes through the sample transfer tube (lefthand side of the figure), and decreased around 35 m/s in the expansion tube (righthand side of the figure).

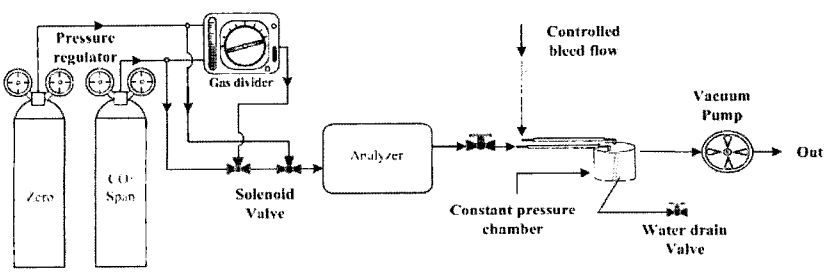

Figure 2. Schematic diagram of the test bench to measure a response time.

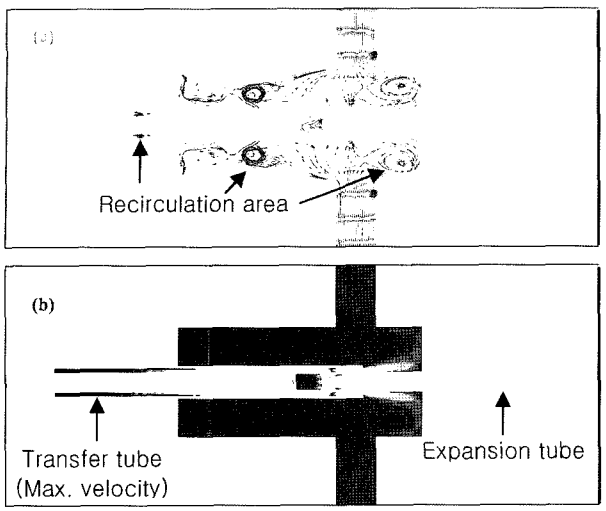

Figure 3. Profiles of (a) streamline and (b) Ma (Mach number) of the fast sampling module with the pressures of the CP chamber - 0.5 bar and optical cell - 0.4 bar.

The recirculation area is observed at the outlet of the transfer tube and the inside of the optical cell. A complicated three dimensional recirculation area of low velocity occurs in several places in the CP chamber. Considering the amount of gas transfered to the sampling module, some of sampled CO_2 gas flows into the CP chamber, and majority of the gas passes through the optical cell and exhausts. The CP chamber at the inlet of optical tube controls flow toward the optical cell properly. As the difference of pressure between the CP chamber and the

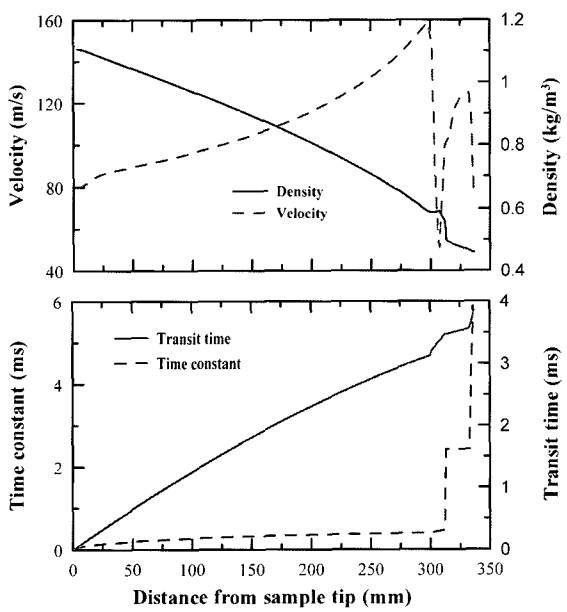

Figure 4. Calculated time constant based on velocity and density of sample gas.

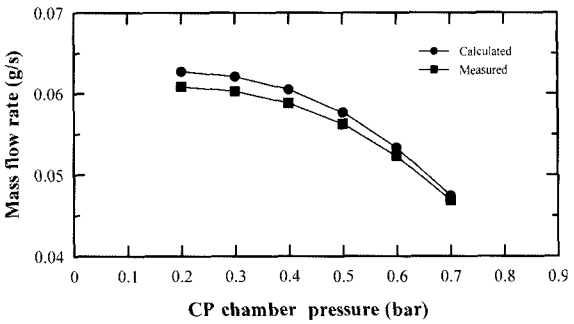

Figure 5. Comparison of modeled and measured mass flow rates of the sampling module.

CP tube is about 0.1 bar, the constant pressure in the expansion tube is well maintained at the inlet of the optical tube hole.

Response time is calculated based on velocity and density distribution, and is illustrated in Figure 4. In the same way, response time prediction is carried out including variation of driving conditions, such as pressure variation of the CP chamber.

5.2. Determination of Operating Range of Sampling Module

Numerical analysis is compared to experimental data in order to ensure the reliability before determining detecting limits. There is a 0.5~4.0% difference of mass flow rate in Figure 5, where the pressure of sample gas is 1 bar. This error grows as the difference of the pressure between sample gas and CP chamber increases due to lack of consideration on entrance effect at the capillary inlet.

Figure 6 shows the mass flow rate of the sample gas,

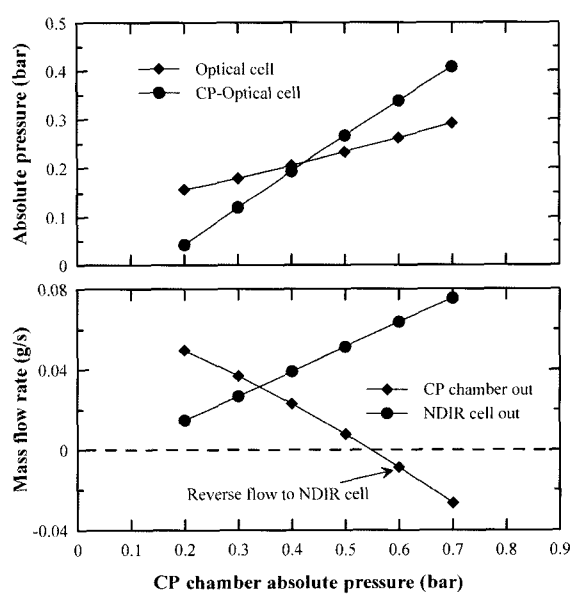

Figure 6. Simulation results for mass flow rate and cell pressure.

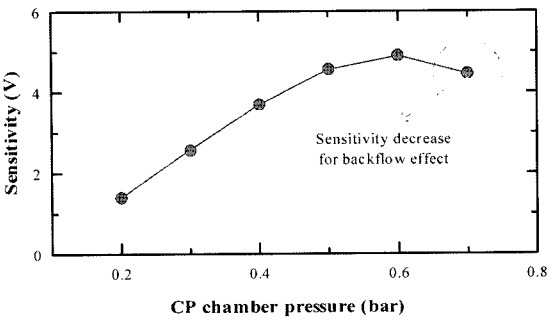

Figure 7. Measured sensitivity with variation of CP chamber pressure.

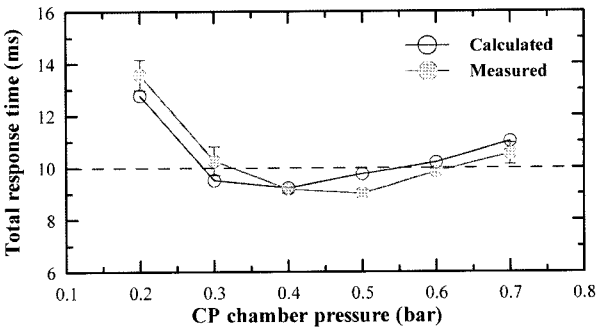

Figure 9. Comparison of total response time with the variation of the CP chamber pressure.

flowing out from the CP chamber with the pressure variation of the CP chamber, as well as the mass flow rate flowing in the optical cell through the optical tube. According to the result from FLUENT, reversed flow is observed when pressure of the CP chamber is 0.6 bar and 0.7 bar.

In other words, since the mass flow rate of the sample gas flowing into the transfer tube is less than the mass flow rate into the optical cell, it can reversely flow into the CP chamber through the bleed line that is installed to control the pressure of the CP chamber.

This phenomenon is also seen by the measured sensitivity from the detector, which shows a defined voltage change, with a change of CO_2 concentration from 0 to 20%. Figure 7 shows that sensitivity decreases when the pressure of the CP chamber is near 0.6 bar and tends to be reversed when the pressure reaches 0.7 bar. Flow toward the optical cell is increasing, whereas flow from the transfer tube is decreasing when the pressure of the CP chamber increases. In other words, this results from decreased CO_2 density flowing into the optical tube from the CP chamber.

Figure 8 is the result of numerical analysis of the amount of sample gas flow passing through the sampling module when the fast analyzer is applied to an intake and exhaust manifold. The use of the sampling modeling could be restricted, depending on the sample gas pressure.

In other words, when the gas pressure is 0.3 bar, reverse flow may occur depending on the pressure of the CP chamber and the optical chamber. According to the results obtained, the sampling module can generate reversed flow when the CP chamber is more than 0.6 bar or the sample gas pressure is less than 0.3 bar. Hence, the operating range of the sampling module should be carefully decided when applied to a practical engine.

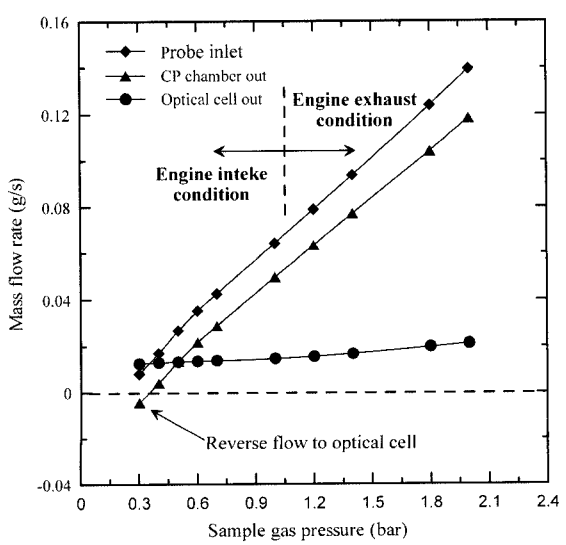

Figure 8. Mass flow rates vs. sample gas pressures.

5.3. Measurement of Analyzer Response Time

There are two parts composing the response time of the concentration analysis: transit time and time constant. Transit time is generally considered the time duration when the gas concentration changes from 0 to 10% and time constant represents time duration to detect the change in gas concentration from 10 to 90%. Transit time can be calculated for a particle to travel from the inlet of the tube to the detector; that is, when the Lagrangian method and time constant calculated for the number of particles flowing into the detector increases from 10 to 90%.

Figure 9 shows the comparison of the response time with variation of the CP chanmber pressure.

Experimental data include variations shown with error bars; note the pressure of CP chamber at 0.2, 0.3, and 0.7 bar, yet within an acceptable error range.

Our analytical estimation agrees well with measured data. According to these results, reliability of the analysis, using a commercial code is verified for compressible flow where the Mach number is above 0.3. An available range for the sampling module is also examined and useful basic data to determine design factors is acquired through numerical analysis.

6. CONCLUSIONS

A new design method for the fast gas sampling is introduced and the numerical analysis by FLUENT is performed to predict internal flow of sampling gas and to determine the available range. Reliability of numerical analysis is verified by comparing with measured response time. Results are summarized as follows.

(1) Flow analysis of the whole sampling module shows distribution of velocity, density and recirculation area in each module. The static pressure at the outlet of the expansion tube and inlet of optical tube is maintained constant, which is one of the design points of the sampling module.

(2) According to the analysis of internal flow distribution and experimentally measured sensitivity, the sampling module can be operated properly when the pressure of the CP chamber is less than 0.6 bar.

(3) It is expected that the sampling module can be successfully applied to the intake manifold of an engine where the pressure drops seriously if the intake manifold pressure is higher than 0.3 bar.

(4) The numerical analysis and experiments show that the total response time can be reduced to 8ms, which is fast enough for real time measurements of exhaust gas, including CO and CO_2 with the NDIR method.

ACKNOWLEDGEMENT–This work was supported by Ajou University and grant No. R01-2006-000-11264-0 from the Basic Research Program of the Korea Science & Engineering Foundation.

REFERENCES

Green, R. M. (2000). Measuring the cylinder-to-cylinder EGR distribution in the intake of diesel engine during transient operation. *SAE Paper No.* 2000-01-2866.

Kim, W. S. (2004). *A Study on Design of Fast Response CO_2 Concentration Analyzer and its Application to Automotive Engine*. Ph.D. Dissertation. Ajou University. Korea.

Lee, S. W., Kim, W. S., Lee, J. H., Park, J. I. and Yoo, J. S. (2006). Measurement of CO_2 concentration and A/F ratio using fast NDIR analyzer on transient condition of SI engine. *Int. J. Automotive Technology* **7, 4,** 385–390.

Peckham, M. (1993). *Study of Engine Wall Layer Hydrocarbons with a Fast Response FID*. Ph.D. Dissertation. Cambridge University. Cambridge. UK.

Sergei, S., Collings, N., Hands, T., Peckham, M. and Burrell, J. (1998). Fast response NO/HC measurements in the cylinder and exhaust port of a DI diesel engine. *SAE Paper No.* 980788.

Summers, T. and Collings, N. (1995). Modeling the transit time of a fast response flame ionisation detector during in-cylinder sampling. *SAE Paper No.* 950160.

Sutela, C., Collings, N., and Hands, T. (2000). Real time CO_2 measurement to determine transient intake gas composition under EGR conditions. *SAE Paper No.* 2000-01-2953.

Zhao, H. and Ladommatos, N. (1999). *Engine Combustion Instrumentation and Diagnostics*. SAE International.